

# Electro-hydraulic Rolling Soft Robot

Khoi Ly



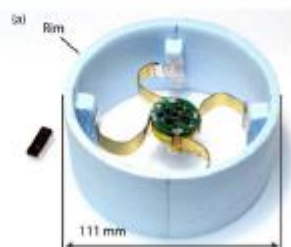
## Shift of Center of Mass



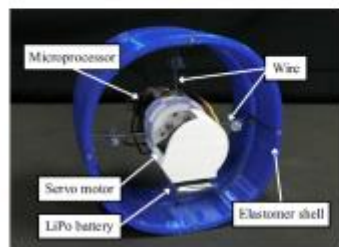
(Xueli et. al., 2014)



(Nguyen et. al., 2017)

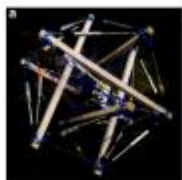


(Must, 2015)

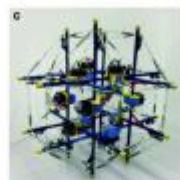


(Masuda, 2017)

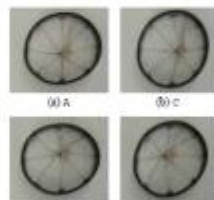
## Geometry Deformation



(Kim et. al., 2020)



(Chiu et. al., 2018)

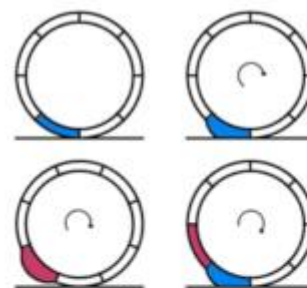


(Sugiyama, 2008)

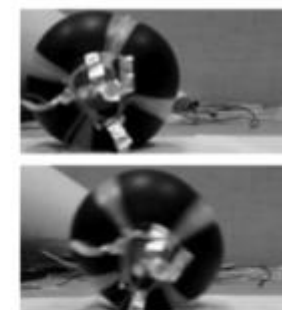
## Shell Bulging



(Correll et. al., 2010)



(Wait et. al., 2010)

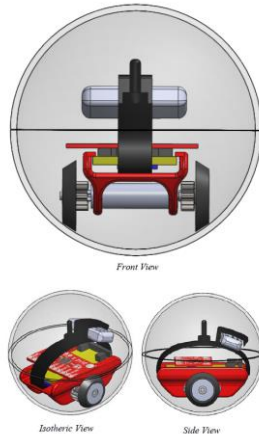


(Potz et. al., 2010)

- Lack system integration
- Lack modeling
- Lack speed regulator

Ly, et. al. (In preparation)

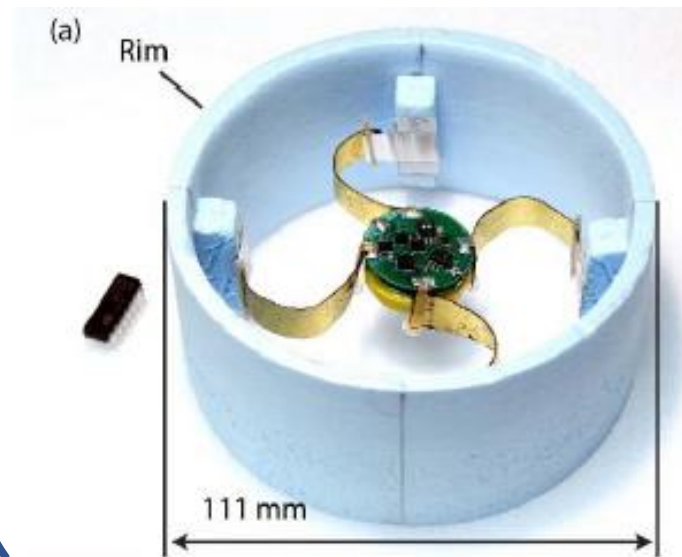
# Shift of Center of Mass



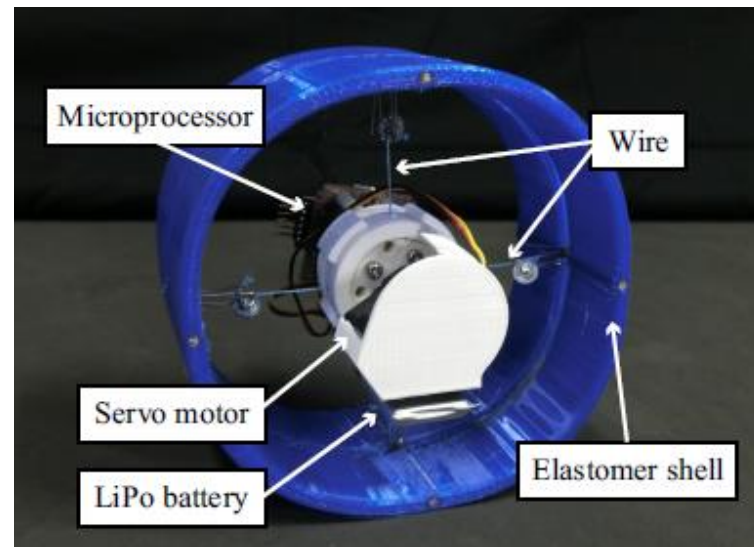
(Xuelel et. al., 2014)



(Nguyen et. al., 2017)

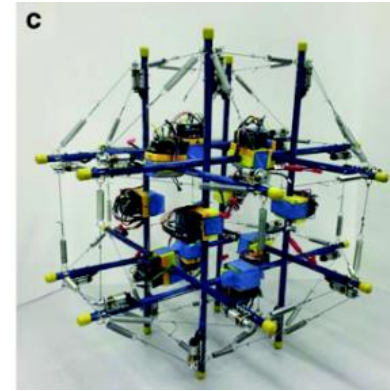
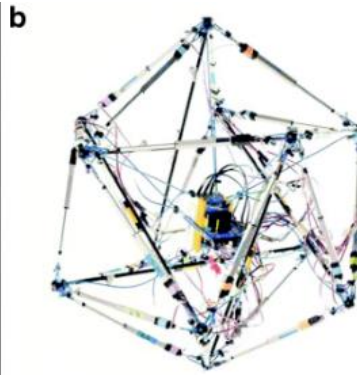
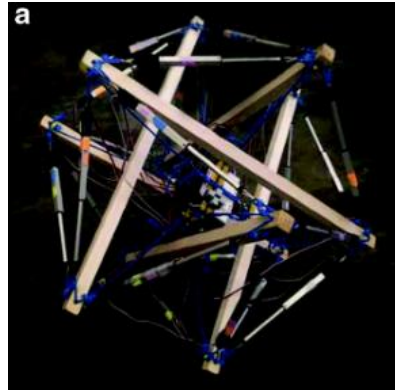


(Must, 2015)

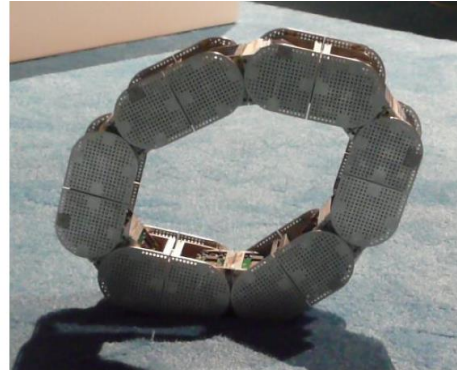
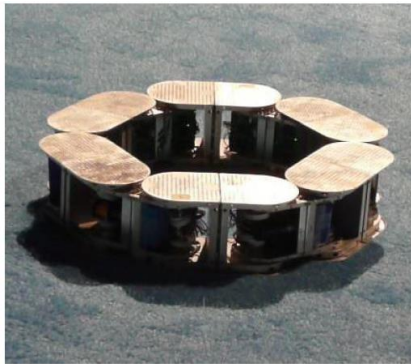


(Masuda, 2017)

# Geometry Deformation



(Kim et. al., 2020)



(Chiu et. al., 2018)



(a) A



(b) C



(c) E

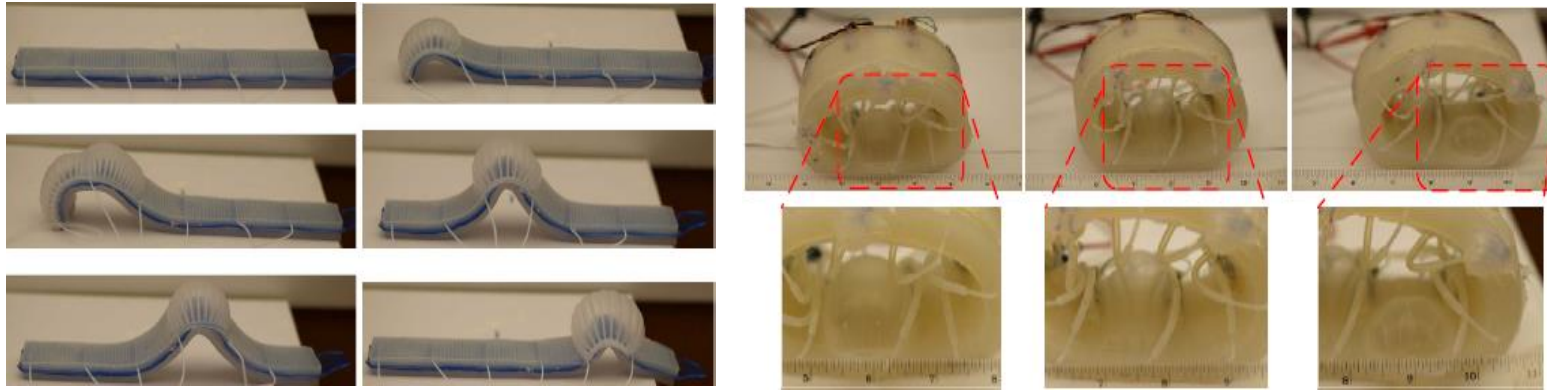


(d) G

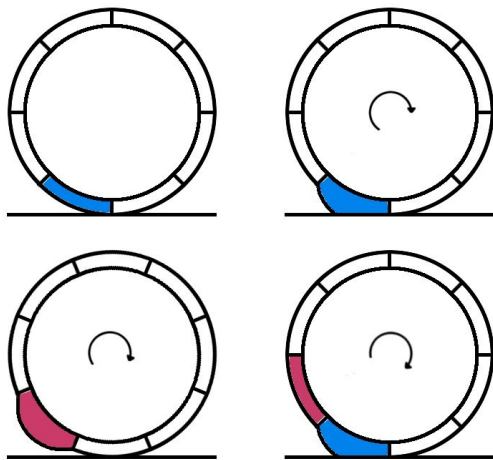
(Sugiyama, 2006)



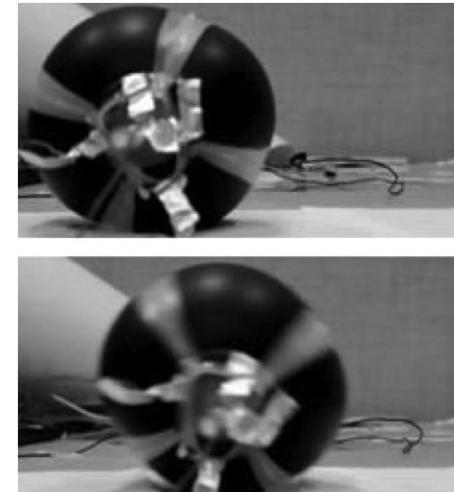
# Shell Bulging



(Correll et. al., 2010)

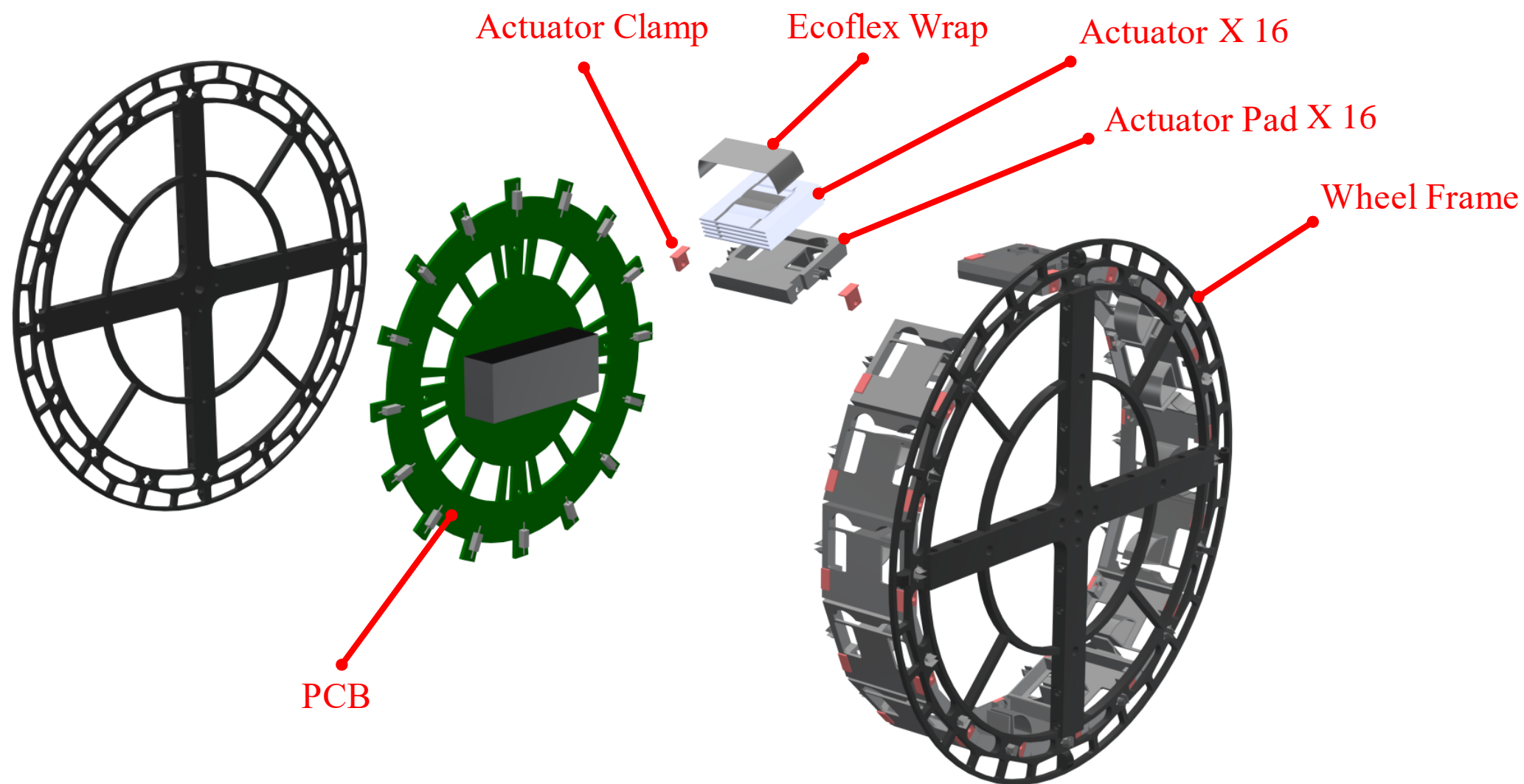


(Wait et. al, 2010)



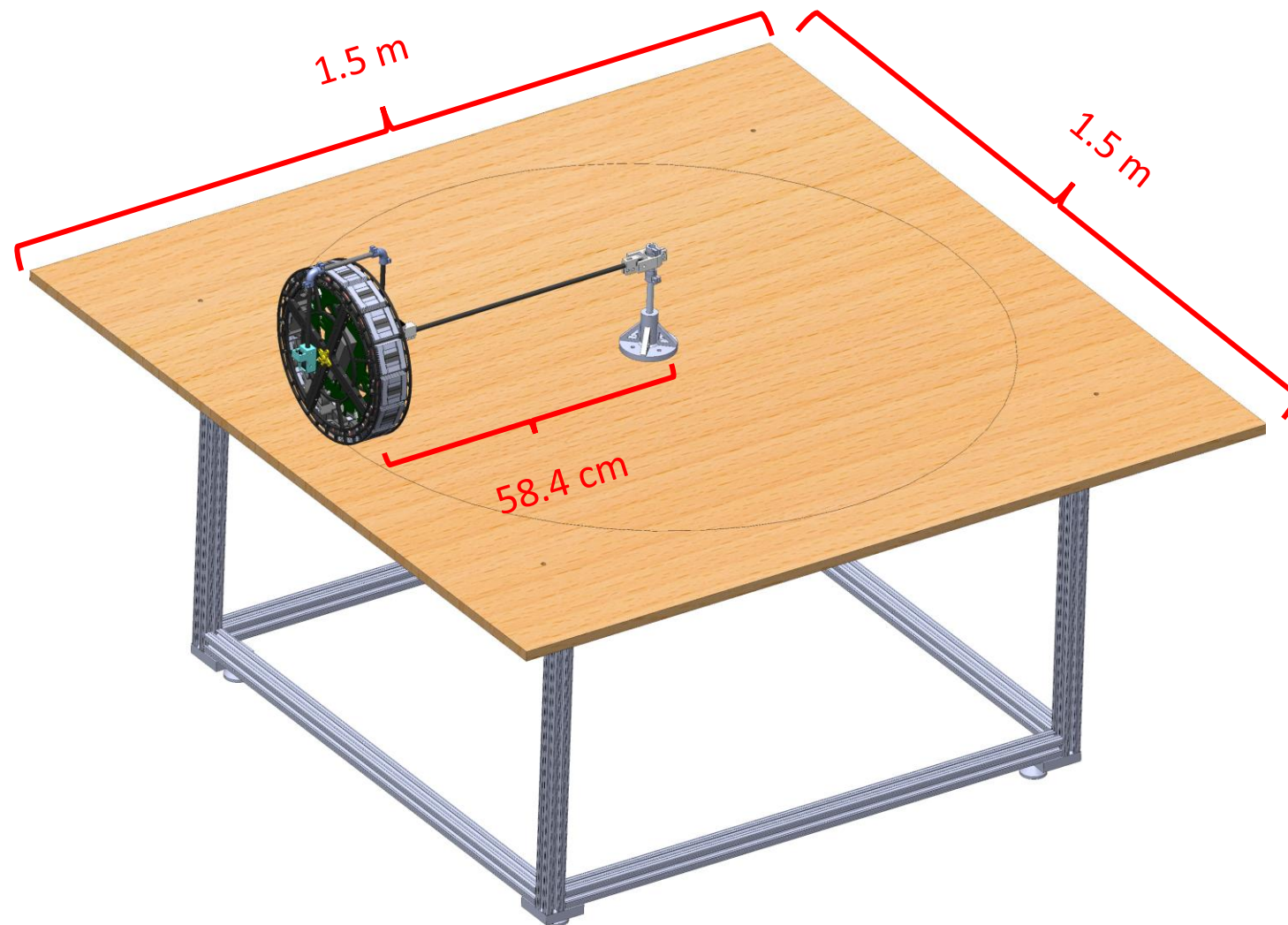
(Potz et. al., 2010)

# 1. Mechanical Design



Ly, et. al. (In preparation)

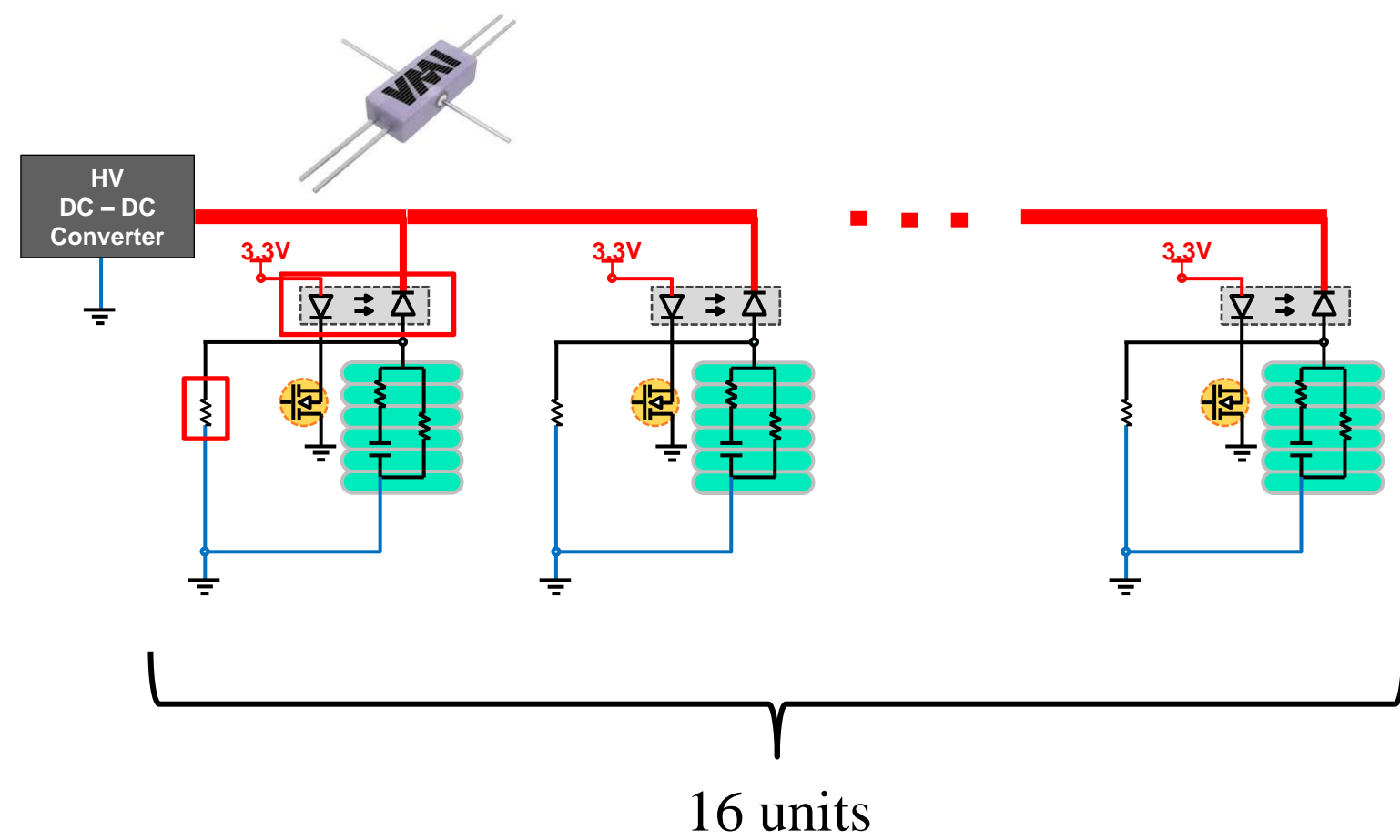
# 1. Mechanical Design



Ly, et. al. (In preparation)



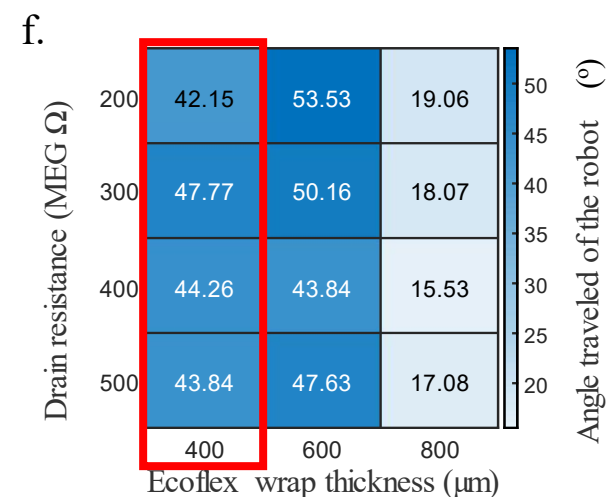
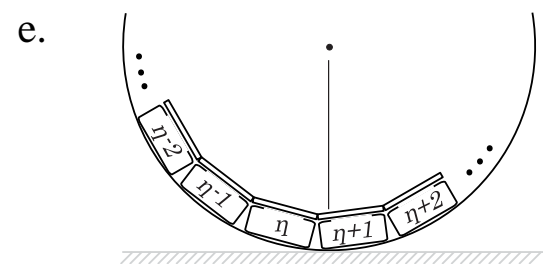
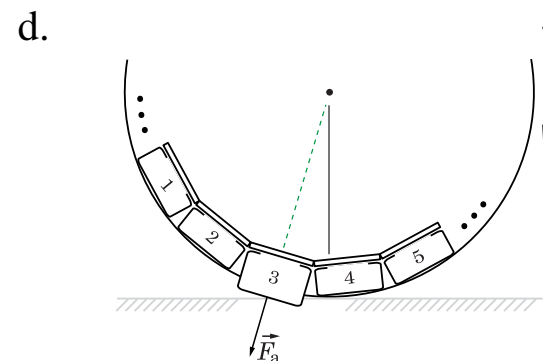
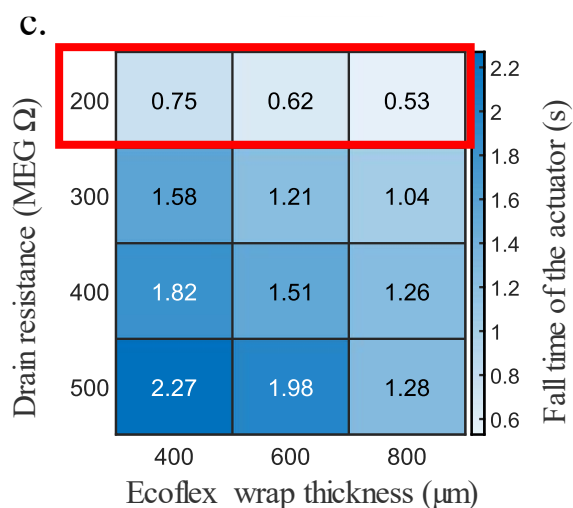
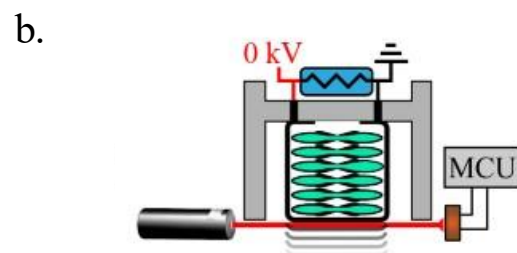
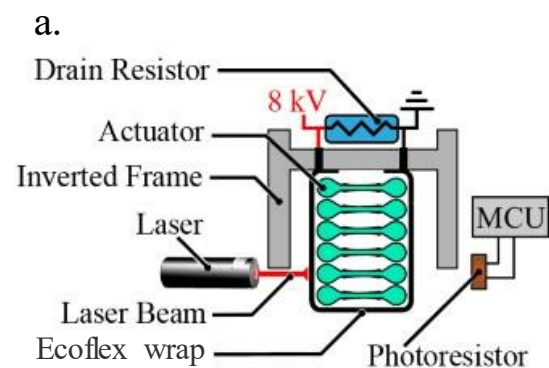
# 2. Electrical Design



Ly, et. al. (In preparation)

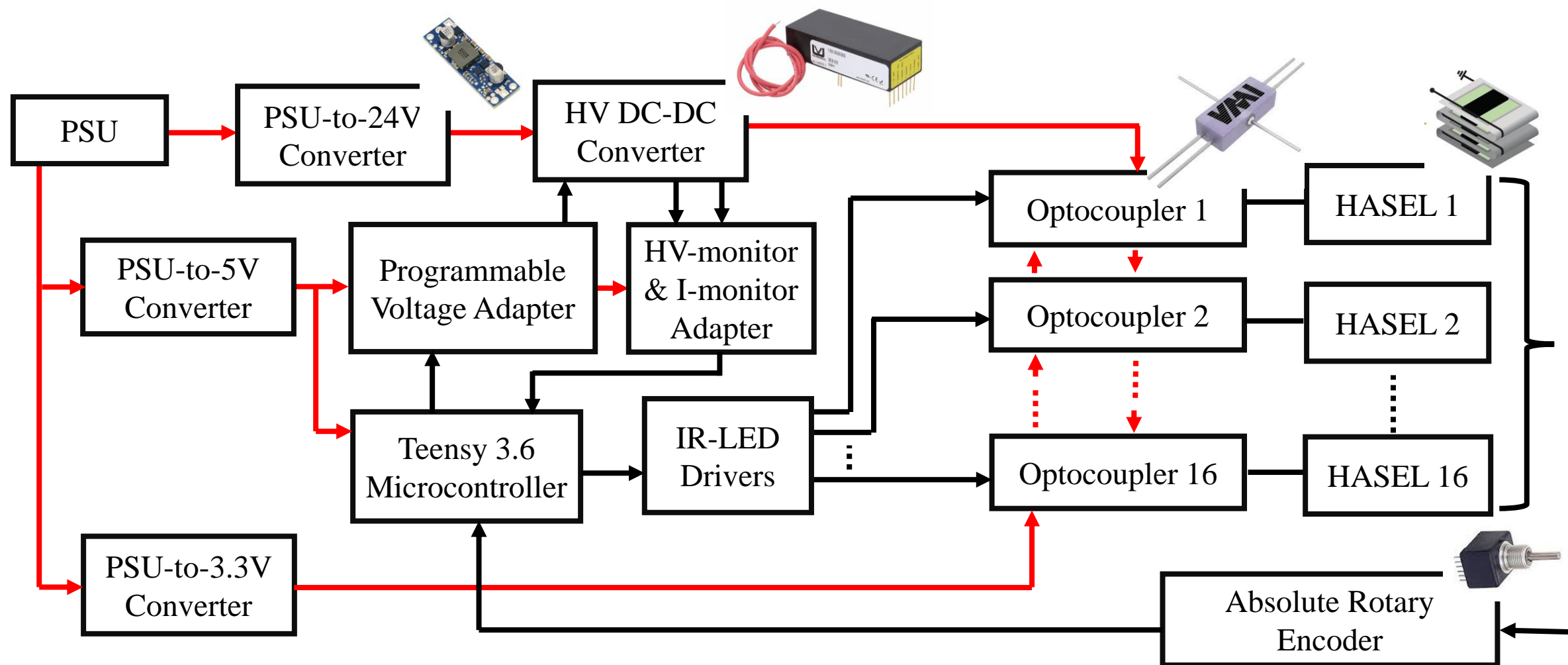


## 2. Electrical Design



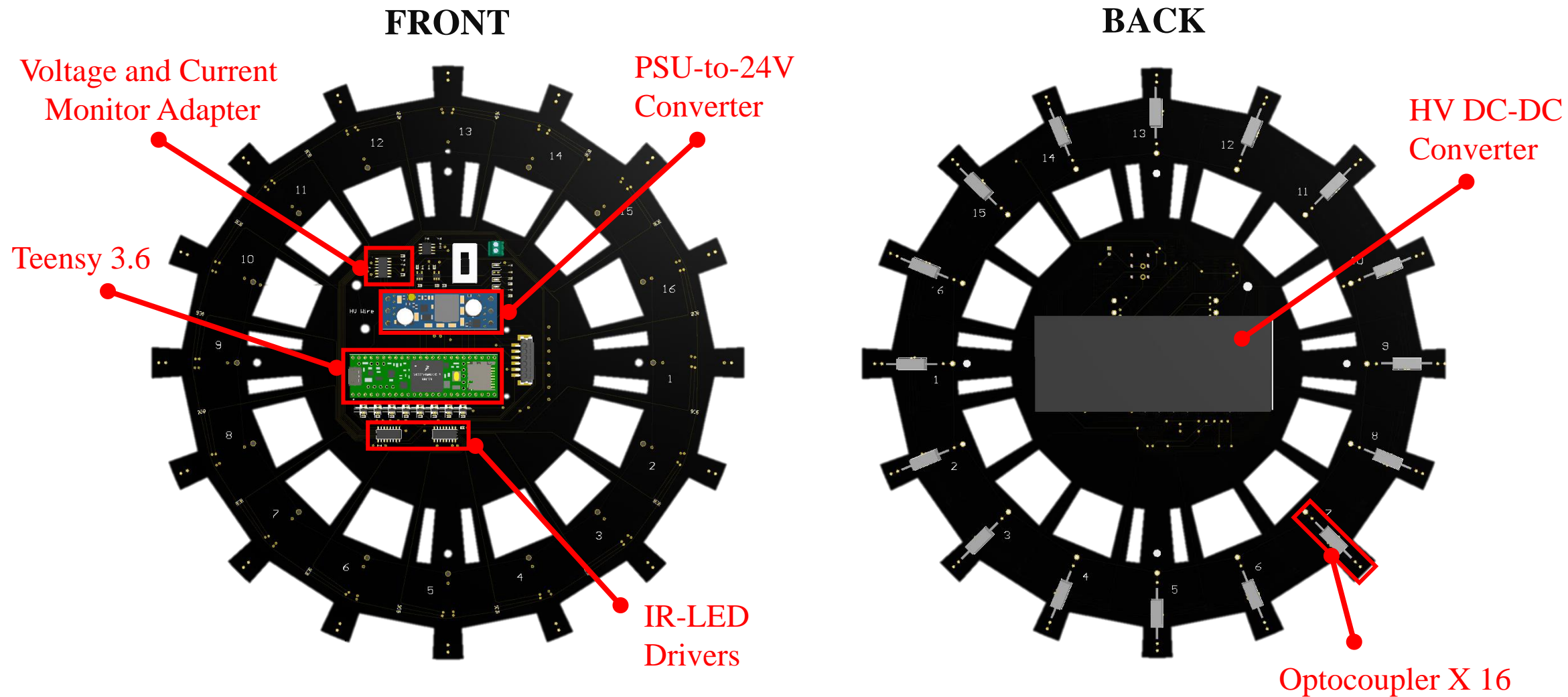
Ly, et. al. (In preparation)

## 2. Electrical Design

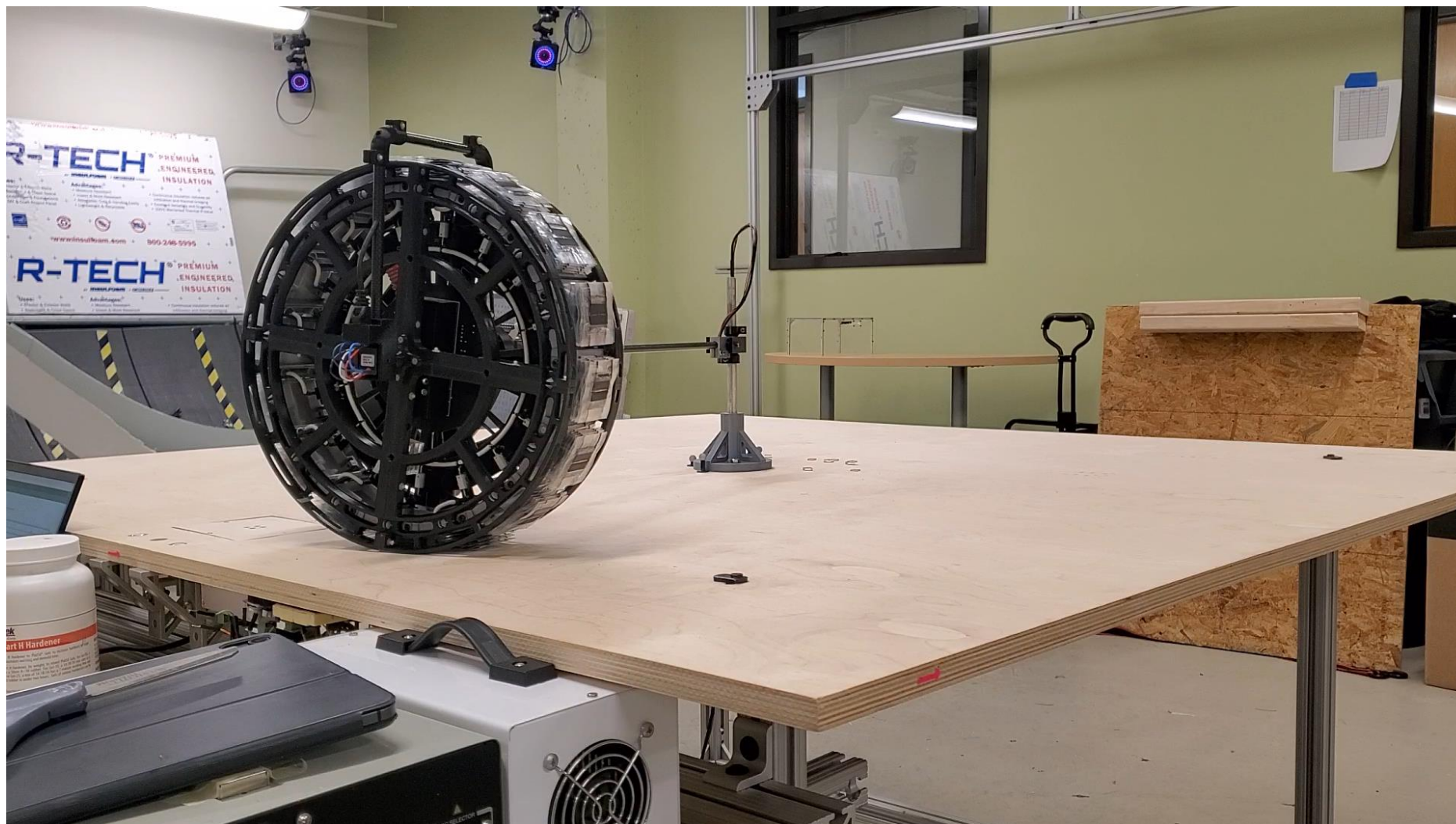


Ly, et. al. (In preparation)

## 2. Electrical Design



Ly, et. al. (In preparation)

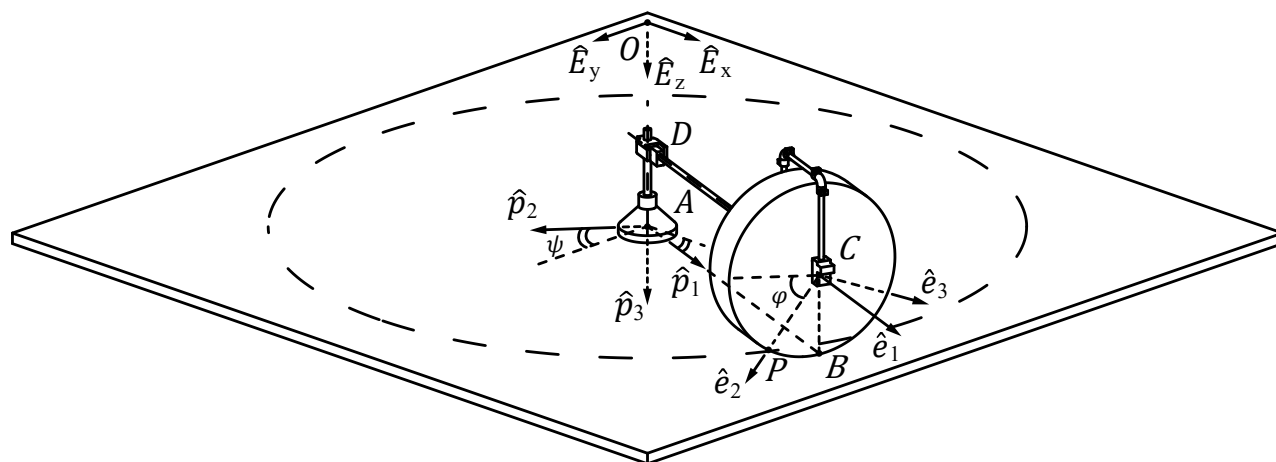


**MARK 8**

Ly, et. al. (In preparation)



# 1. Dynamics modeling of the rolling robot



Assumption  ${}^F\vec{v}_B^{\mathcal{R}} = \vec{0}$

Velocity of the Robot's Center of Mass (point C)

- Platform-fixed frame  $\mathcal{F}: \{\hat{E}_x, \hat{E}_y, \hat{E}_z\}$
- The reference frame  $\mathcal{P}: \{\hat{p}_1, \hat{p}_2, \hat{p}_3\}$
- The reference frame  $\mathcal{R}: \{\hat{e}_1, \hat{e}_2, \hat{e}_3\}$

$${}^F\vec{v}_C = {}^F\vec{v}_B^{\mathcal{R}} + {}^F\vec{\omega}^{\mathcal{R}} \times (\vec{r}_C - \vec{r}_B)$$

$$\Rightarrow {}^F\vec{v}_C = r\dot{\phi}\hat{p}_2$$

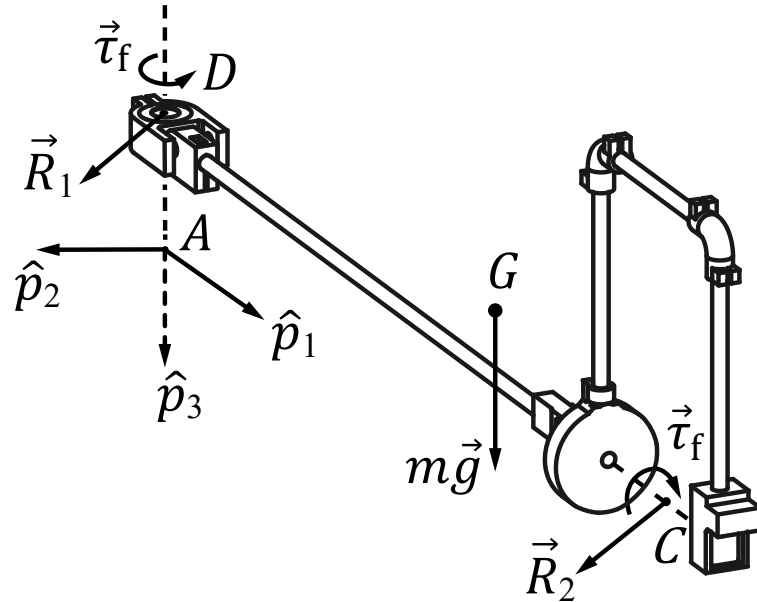
$${}^F\vec{v}_C = {}^{\mathcal{P}}\frac{d}{dt}(\vec{r}_C) + {}^F\vec{\omega}^{\mathcal{P}} \times \vec{r}_C$$

$$\Rightarrow {}^F\vec{v}_C = \dot{\psi} L \cdot \hat{p}_2$$

$$\dot{\psi} = \frac{r}{L}\dot{\phi}$$

Ly, et. al. (In preparation)

# 1. Dynamics modeling of the rolling robot



Only rotational motion

$$\vec{M}_D = \frac{d}{dt}({}^{\mathcal{F}}\vec{H}_D)$$

$$\begin{aligned} 0 &= I_{13} \ddot{\psi} - I_{23} \dot{\psi}^2 \\ -m g x_{GA} - L R_{23} &= I_{23} \ddot{\psi} + I_{13} \dot{\psi}^2 \\ L R_{22} - \tau_f &= I_{33} \ddot{\psi} \end{aligned}$$

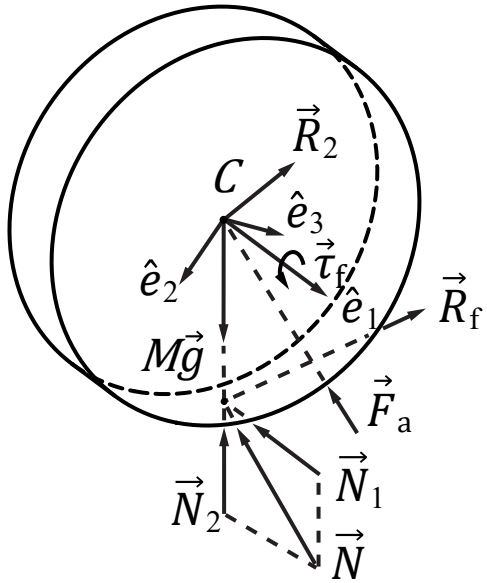
$\begin{bmatrix} I_{11} & I_{12} & I_{13} \\ I_{21} & I_{22} & I_{23} \\ I_{31} & I_{32} & I_{33} \end{bmatrix}$ : Inertia Tensor matrix for the pivot arm and U-mount

$L$ : Distance between the pivot center (A) and the robot's COM (C)

$G$ : COM of the pivot arm and U-mount

Ly, et. al. (In preparation)

# 1. Dynamics modeling of the rolling robot



## Translational motion

$$\sum \vec{F} = M \cdot {}^{\mathcal{F}}\vec{a}_C$$

$$-R_{21} + N_1 = M r \dot{\psi} \dot{\phi}$$

$$-R_{22} - R_f + F_{a,2} = M r \ddot{\phi}$$

$$Mg - R_{23} + N_3 + F_{a,3} = 0$$

## Rotational motion

$$r R_f - \tau_f = I_1 \ddot{\phi} + (I_3 - I_2) \dot{\psi}^2 \sin(\phi) \cos(\phi)$$

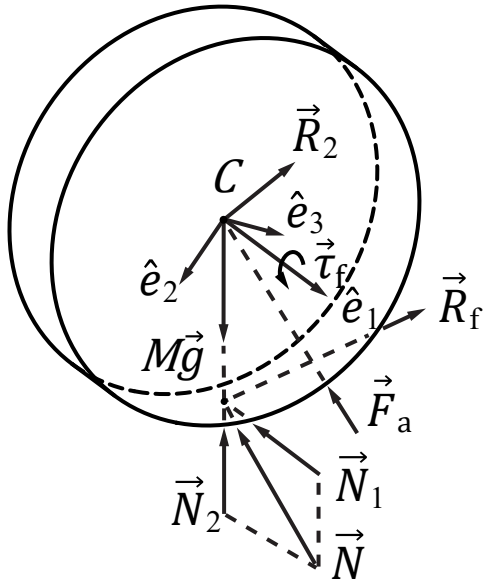
$$\vec{M}_C = {}^{\mathcal{F}}\frac{d}{dt}({}^{\mathcal{F}}\vec{H}_C) \quad r N_1 \cos(\phi) = I_2 (\ddot{\psi} \sin(\phi) + \dot{\psi} \dot{\phi} \cos(\phi)) + (I_1 - I_3) \dot{\psi} \dot{\phi} \cos(\phi)$$

$$-r N_1 \sin(\phi) = I_3 (\ddot{\psi} \cos(\phi) - \dot{\psi} \dot{\phi} \sin(\phi)) + (I_2 - I_1) \dot{\psi} \dot{\phi} \sin(\phi)$$

$$\begin{bmatrix} I_1 & 0 & 0 \\ 0 & I_2 & 0 \\ 0 & 0 & I_3 \end{bmatrix} : \text{Inertia Tensor matrix for the rolling robot}$$

Ly, et. al. (In preparation)

# 1. Dynamics modeling of the rolling robot



$$L r F_2 - r \tau_f - L \tau_f = L I_1 \ddot{\varphi} + r (I_3 - I_2) \frac{I_{13}}{I_{23}} \ddot{\varphi} \sin(\varphi) \cos(\varphi) + \left( L M r^2 + I_{33} \frac{r^2}{L} \right) \ddot{\varphi}$$

$$\left( L I_1 + L M r^2 + I_{33} \frac{r^2}{L} \right) \ddot{\varphi} = L r F_{a,2} - (r \tau_f + L \tau_f) \text{sign}(\dot{\varphi})$$

$$\begin{bmatrix} \dot{\xi}_1 \\ \dot{\xi}_2 \end{bmatrix} = \begin{bmatrix} \xi_2 \\ \frac{1}{L I_1 + L M r^2 + I_{33} \frac{r^2}{L}} \left( L r F_{a,2} - (r \tau_f + L \tau_f) \text{sign}(\xi_2) \right) \end{bmatrix}$$

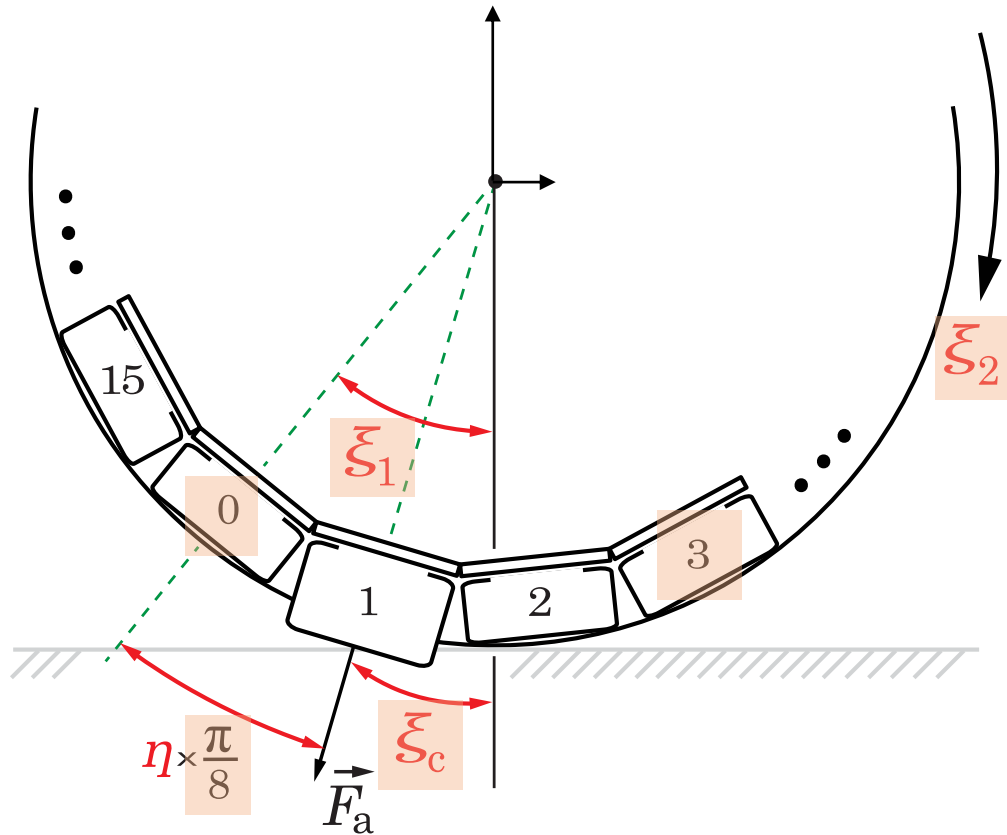
$\xi_1 := \varphi \in \mathbb{R}$  is the angular position of the robot

$\xi_2 := \dot{\varphi} \in \mathbb{R}$  is the angular velocity of the robot

Ly, et. al. (In preparation)



## 2. Hybrid State-space model of the rolling robot



$$u = \begin{bmatrix} n_a \\ \varphi_a \\ \varphi_d \end{bmatrix}$$

- $n_a$ : the target actuator to be activated
- $\varphi_a$ : activation angle
- $\varphi_d$ : deactivation angle

Current actuator index :  $\eta = \lfloor \xi_1 / (\pi/8) \rfloor$

Contact angle of actuator  $\eta^{\text{th}}$  :  $\xi_c = \xi_1 - \eta (\pi / 8)$

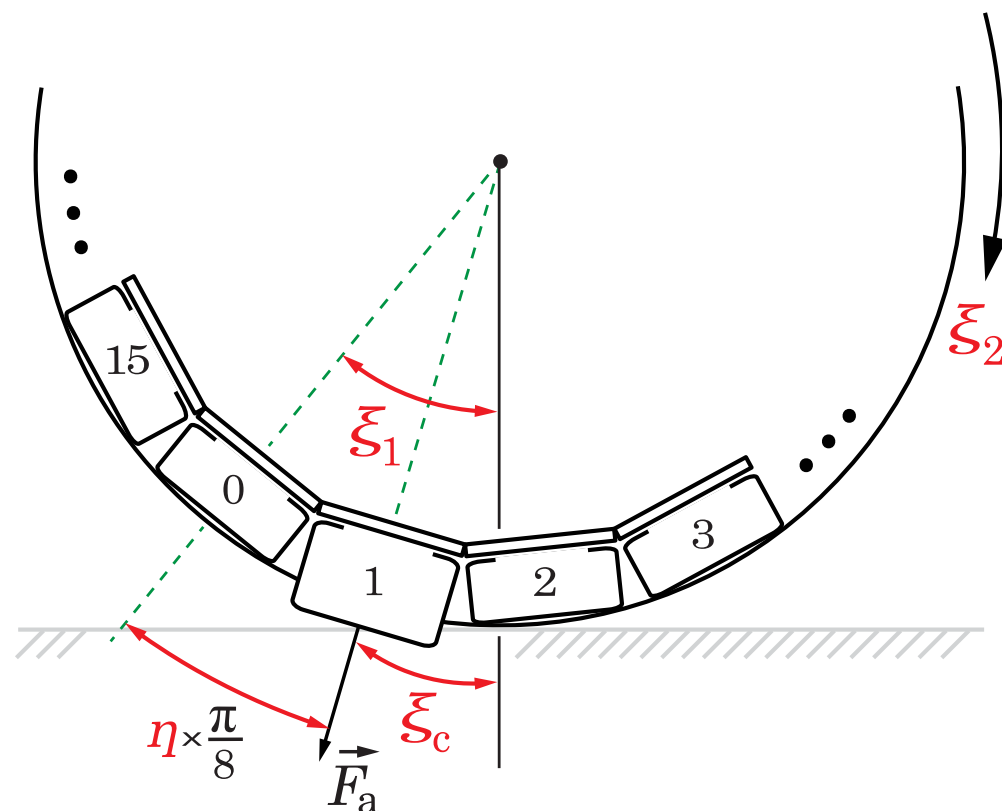
$q \in \{0,1\}$ : where 0 means not activated, 1 means activated

Activation angle down counter:  $\dot{\Delta} = -(1 - q) \xi_2$

Deactivation angle down counter:  $\dot{\delta} = -\xi_2$

Ly, et. al. (In preparation)

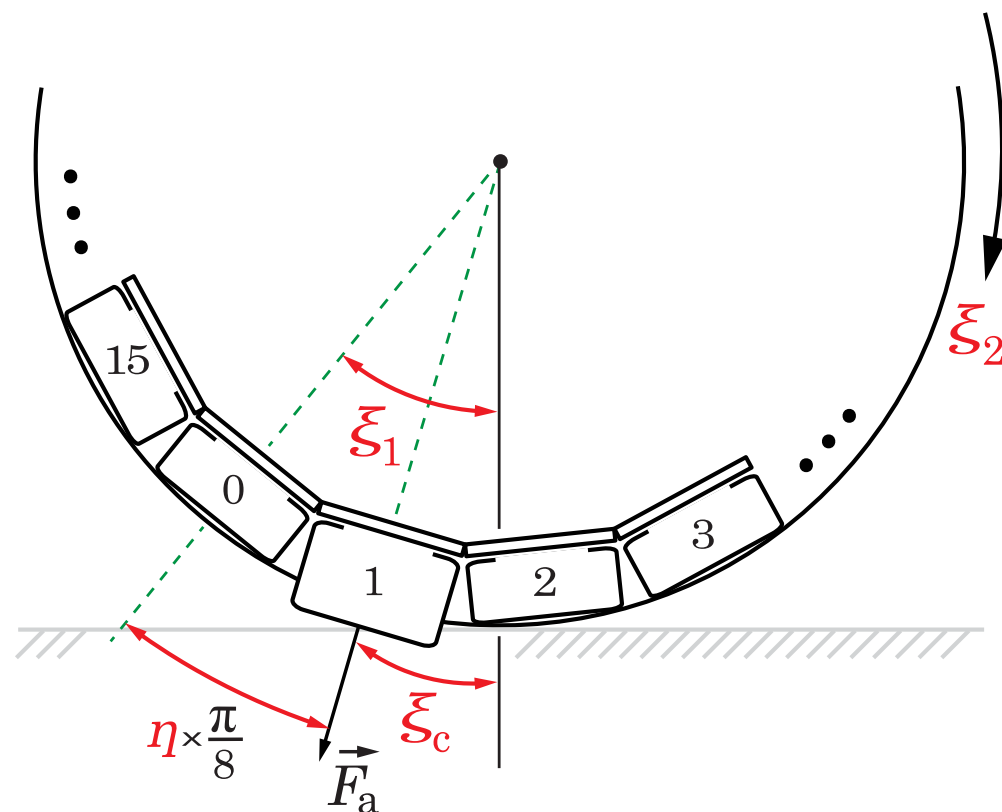
## 2. Hybrid State-space model of the rolling robot



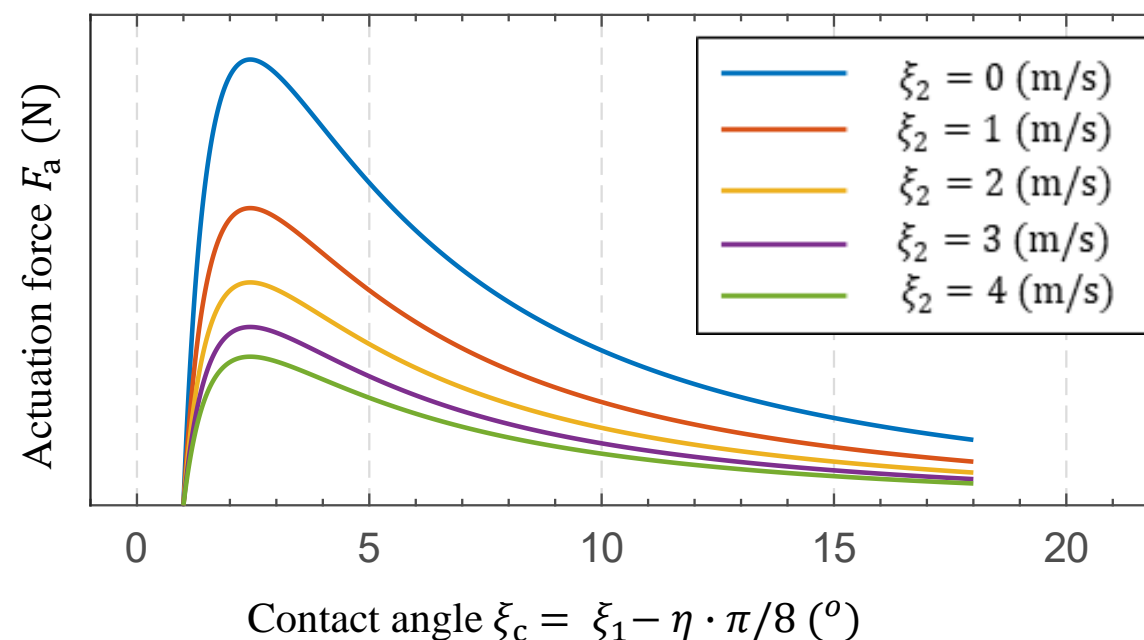
$$f(x, u) = \begin{bmatrix} \dot{\xi}_1 \\ \dot{\xi}_2 \\ \dot{q} \\ \dot{\Delta} \\ \dot{\delta} \\ \dot{\eta} \end{bmatrix} = \begin{bmatrix} \xi_2 \\ \frac{1}{LI_1 + LMr^2 + I_{33} \frac{r^2}{L}} (Lr(F_a \sin(\xi_c) - (r\tau_f + L\tau_f)\text{sign}(\xi_2))) \\ 0 \\ -(1-q)\xi_2 \\ -\xi_2 \\ 0 \end{bmatrix}$$

Ly, et. al. (In preparation)

## 2. Hybrid State-space model of the rolling robot

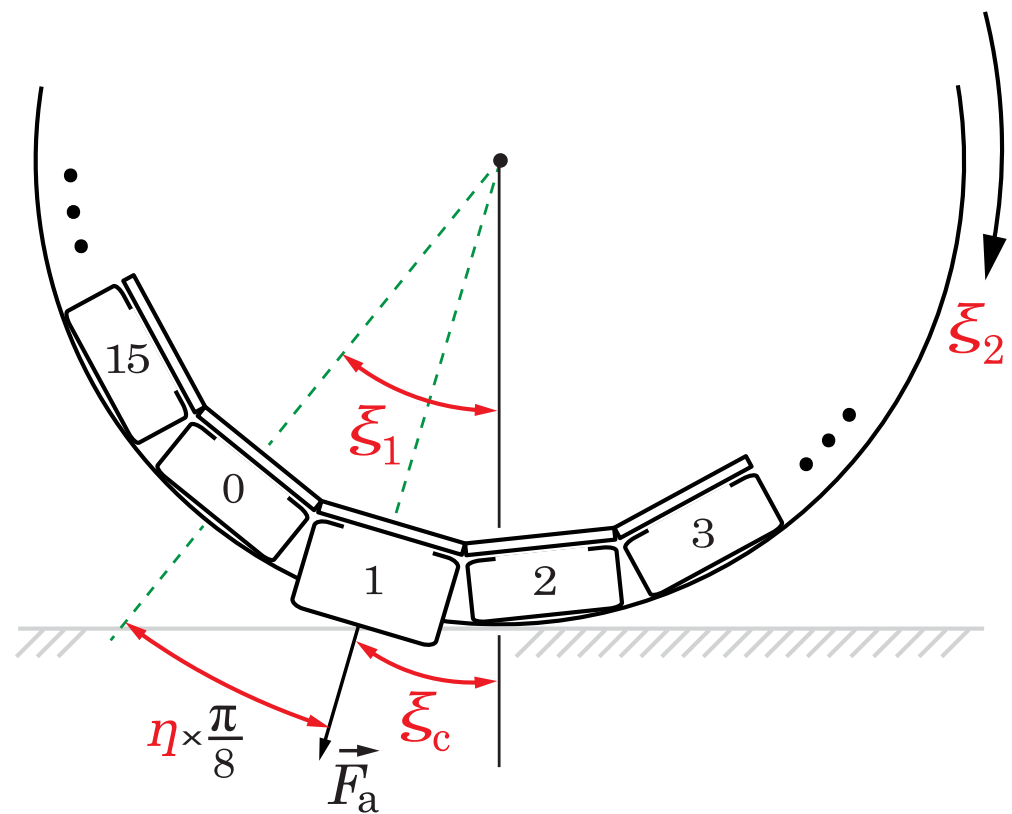


$$F_a(\xi_c, \xi_2, q, \varphi_a) = \frac{1}{\xi_c^{\sigma_1}} \frac{1}{\sigma_2 \xi_2 + \sigma_3} e^{-\frac{(\ln(\xi_c) - \sigma_4)^2}{\sigma_5^2}} q \sigma_6 (\xi_c - \varphi_a)$$



Ly, et. al. (In preparation)

# 2. Hybrid State-space model of the rolling robot



$$\mathcal{H} = (\mathcal{C}, f, \mathcal{D}, g)$$

$$\mathcal{H} = \begin{cases} \dot{x} = f(x, u) \\ x^+ = g(x, u) \\ y = h(x) \end{cases} \quad \begin{array}{l} (x, u) \in \mathcal{C} \\ (x, u) \in \mathcal{D} \end{array}$$

$$q^+ = 1 - q$$

$$\Delta^+ = q \left( \varphi_a + n_a \left( \frac{\pi}{8} \right) - \xi_1 \right)$$

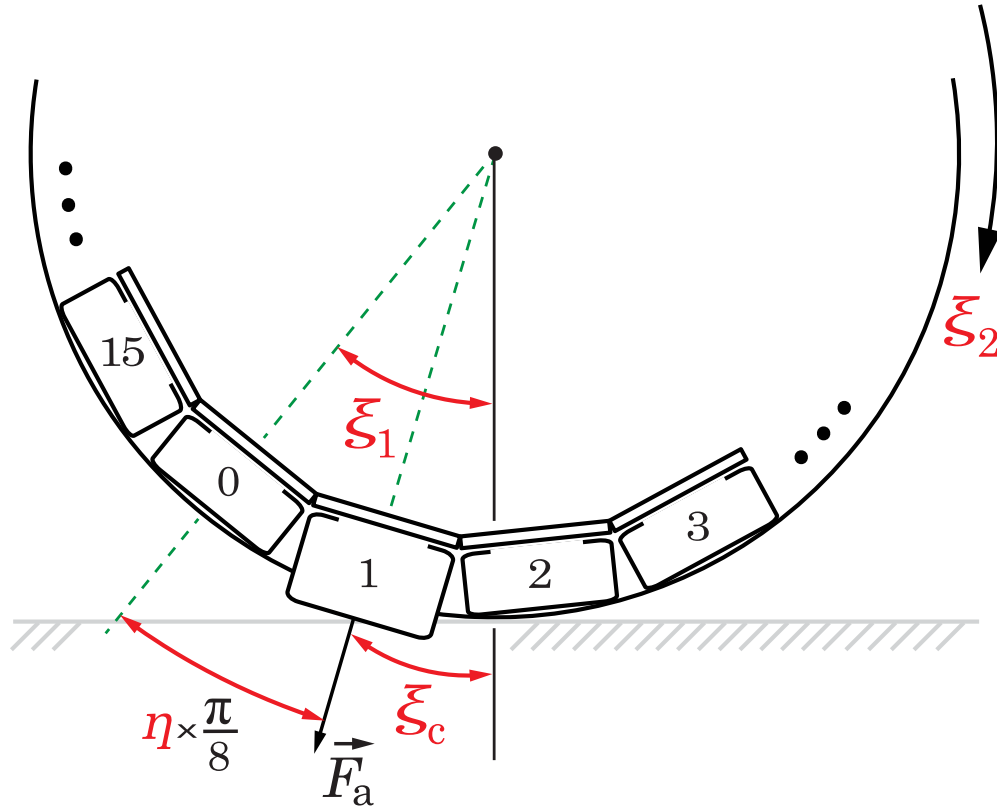
$$\delta^+ = \varphi_d + n_a \left( \frac{\pi}{8} \right) - \xi_1$$

$$\eta^+ = q n_a + (1 - q) \eta$$

Ly, et. al. (In preparation)



## 2. Hybrid State-space model of the rolling robot



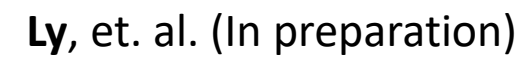
$$\begin{bmatrix} \dot{\xi}_1 \\ \dot{\xi}_2 \\ \dot{q} \\ \dot{\Delta} \\ \dot{\delta} \\ \dot{\eta} \end{bmatrix} = \begin{bmatrix} \xi_2 \\ \frac{1}{LI_1 + LMr^2 + I_{33} \frac{r^2}{L}} (Lr (F_a \sin(\xi_c) - (r\tau_f + L\tau_f) \text{sign}(\xi_2))) \\ 0 \\ -(1-q) \xi_2 \\ -\xi_2 \\ 0 \end{bmatrix}$$

$$\begin{bmatrix} \xi_1^+ \\ \xi_2^+ \\ q^+ \\ \Delta^+ \\ \delta^+ \\ \eta^+ \end{bmatrix} = \begin{bmatrix} \xi_1 \\ \xi_2 \\ 1-q \\ q \left( n_a \left( \frac{\pi}{8} \right) + \varphi_a - \xi_1 \right) \\ n_a \left( \frac{\pi}{8} \right) + \varphi_d - \xi_1 \\ q n_a + (1-q) \eta \end{bmatrix}$$

$$\mathcal{C} := \{x \in \mathbb{R}^2 \times \{0,1\} \times \mathbb{R}^2 \times \mathbb{N}_{\geq 0} \mid \sim(\Delta = 0 \wedge \delta \neq 0 \wedge q = 0) \wedge \sim(\Delta = 0 \wedge \delta = 0 \wedge q = 1)\}$$

$$\mathcal{D} := \{x \in \mathbb{R}^2 \times \{0,1\} \times \mathbb{R}^2 \times \mathbb{N}_{\geq 0} \mid (\Delta = 0 \wedge \delta \neq 0 \wedge q = 0) \vee (\Delta = 0 \wedge \delta = 0 \wedge q = 1)\}$$

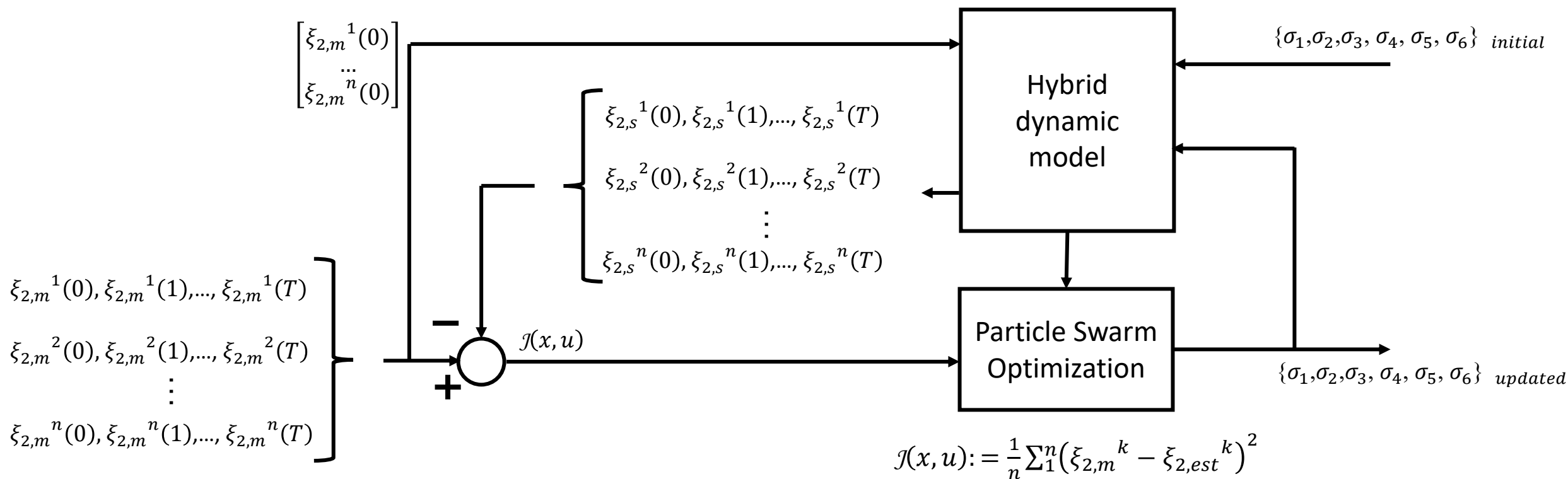
Ly, et. al. (In preparation)



### 3. Estimation of actuation force function based on measured kinematic data

$$u = \begin{bmatrix} n_a = 16 \bmod (\eta + 1) \\ \varphi_a \\ 22^\circ \end{bmatrix}$$

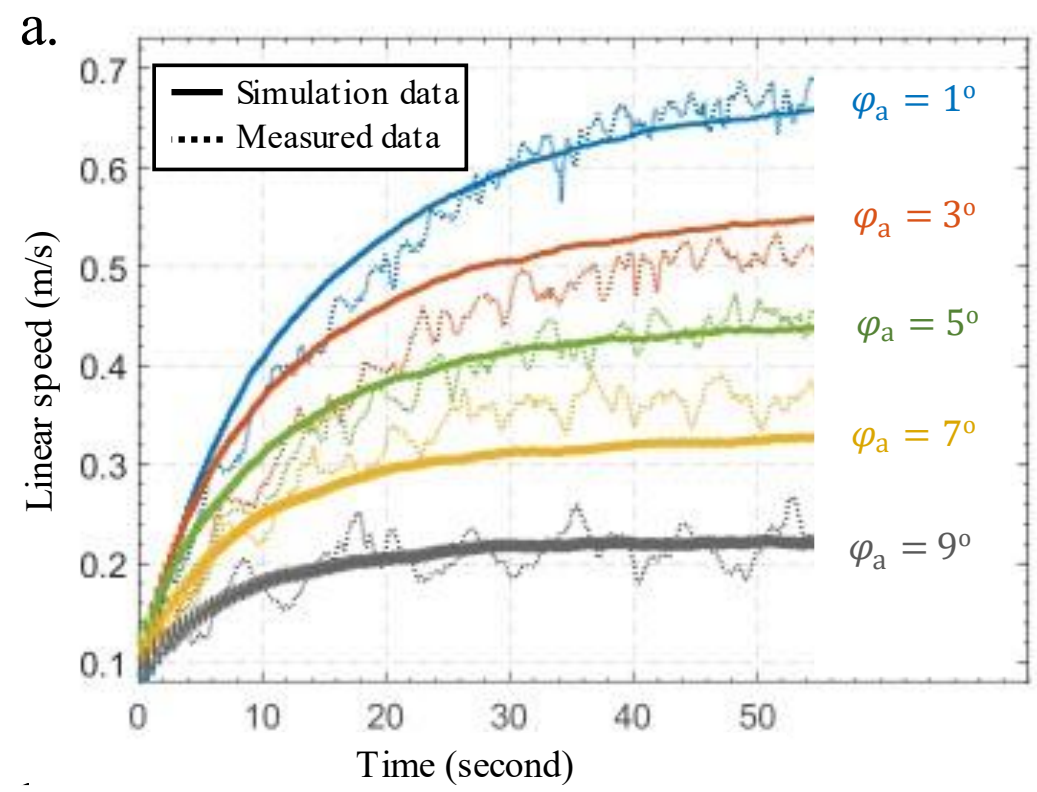
$$F_a(\xi_c, \xi_2, q, \varphi_a) = \frac{1}{\xi_c^{\sigma_1}} \frac{1}{\sigma_2 \xi_2 + \sigma_3} e^{-\frac{(\ln(\xi_c) - \sigma_4)^2}{\sigma_5^2}} q \sigma_6 (\xi_c - \varphi_a)$$



Ly, et. al. (In preparation)

# 4. Evaluation of actuation force function

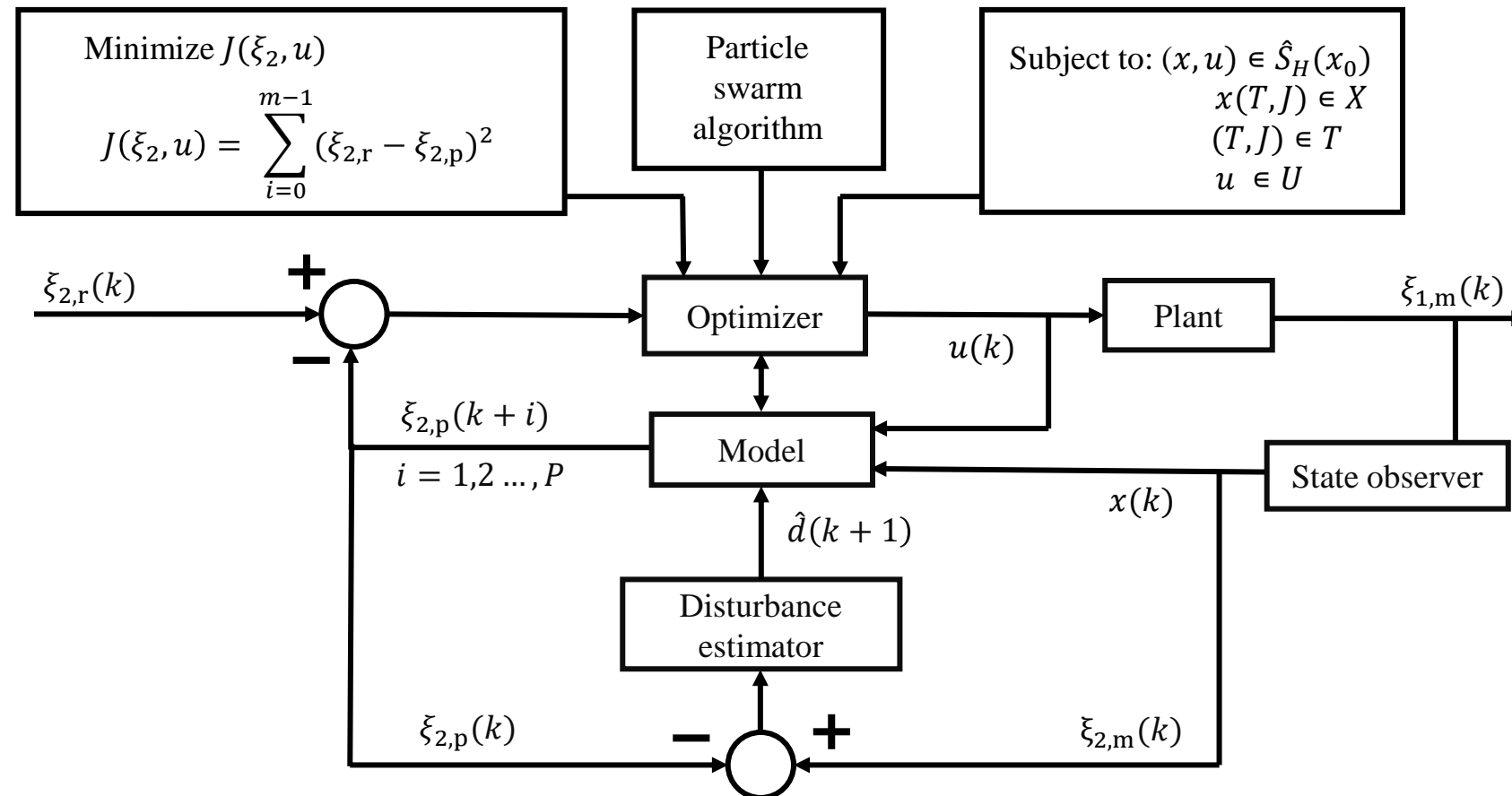
$$\{\sigma_1, \sigma_2, \sigma_3, \sigma_4, \sigma_5, \sigma_6\} = \{1.214, 1.997, 3.836, -1.004, -0.1009, 22.357\}$$



Ly, et. al. (In preparation)

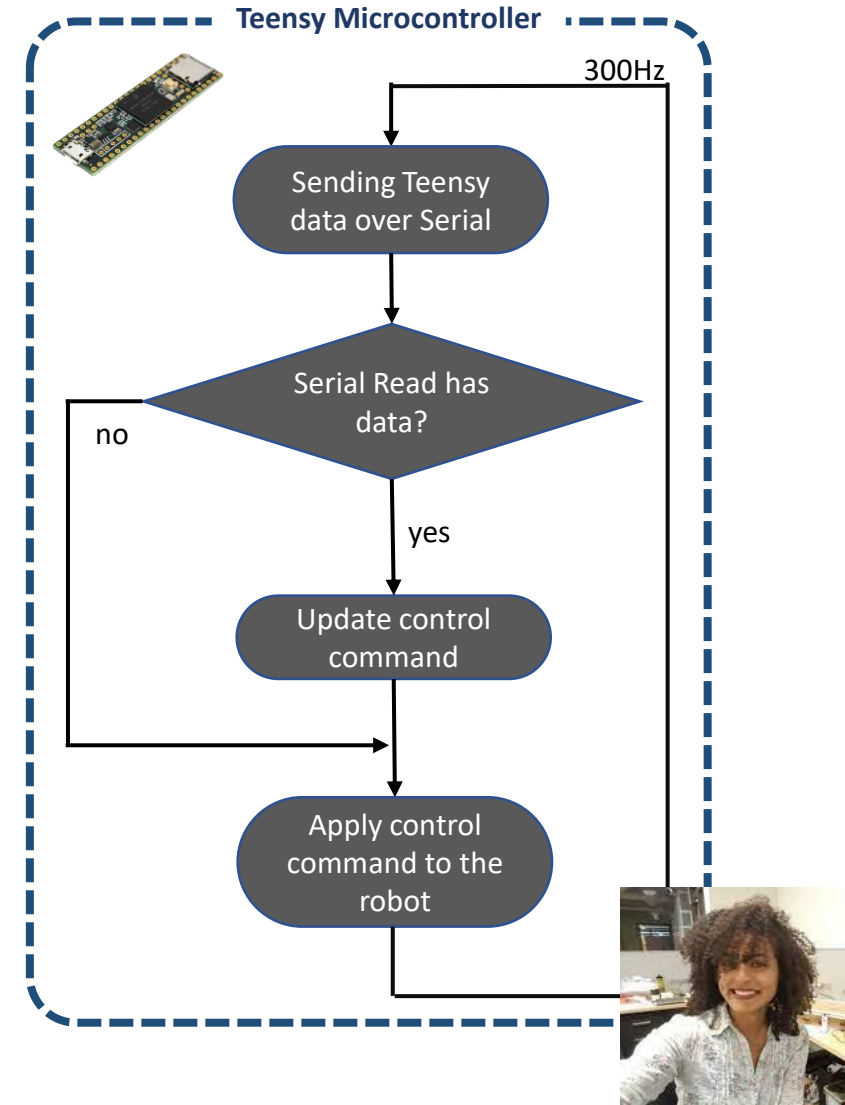
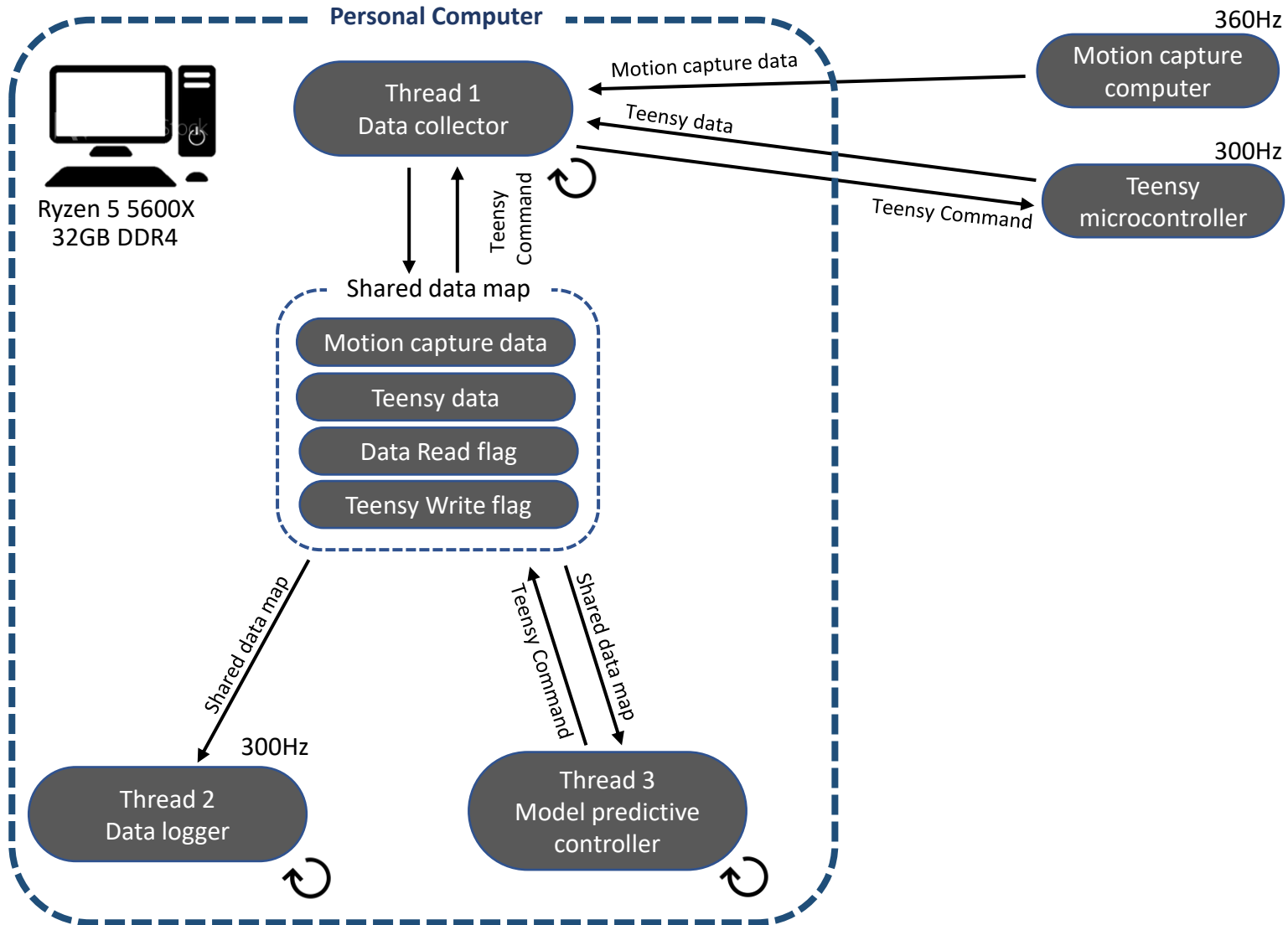


# 1. Description of controller



Ly, et. al. (In preparation)

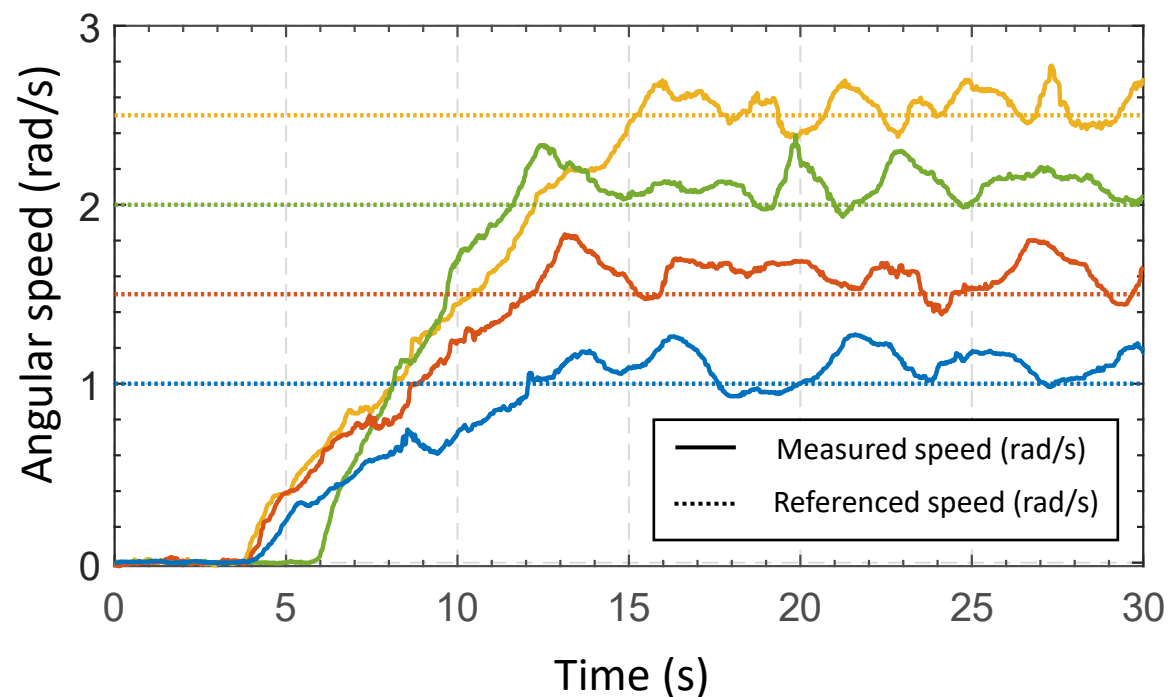
## 2. Real-time, multi-threaded implementation



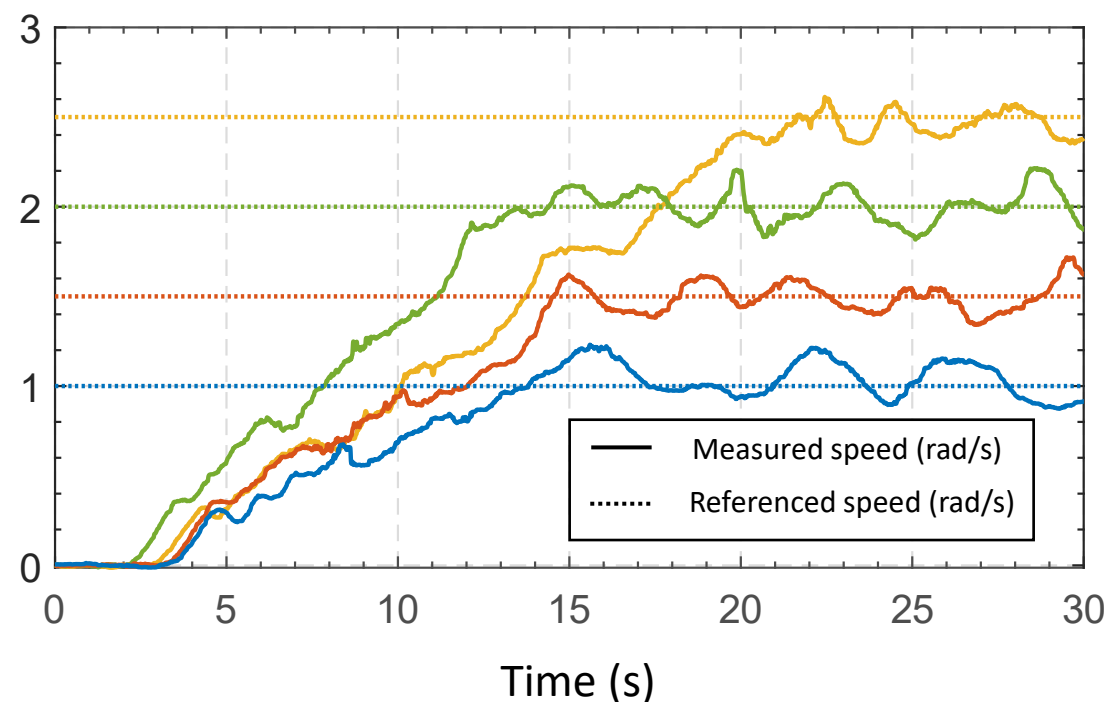
Ly, et. al. (In preparation)

### 3. Preliminary Results

Step Tracking without Disturbance Estimator

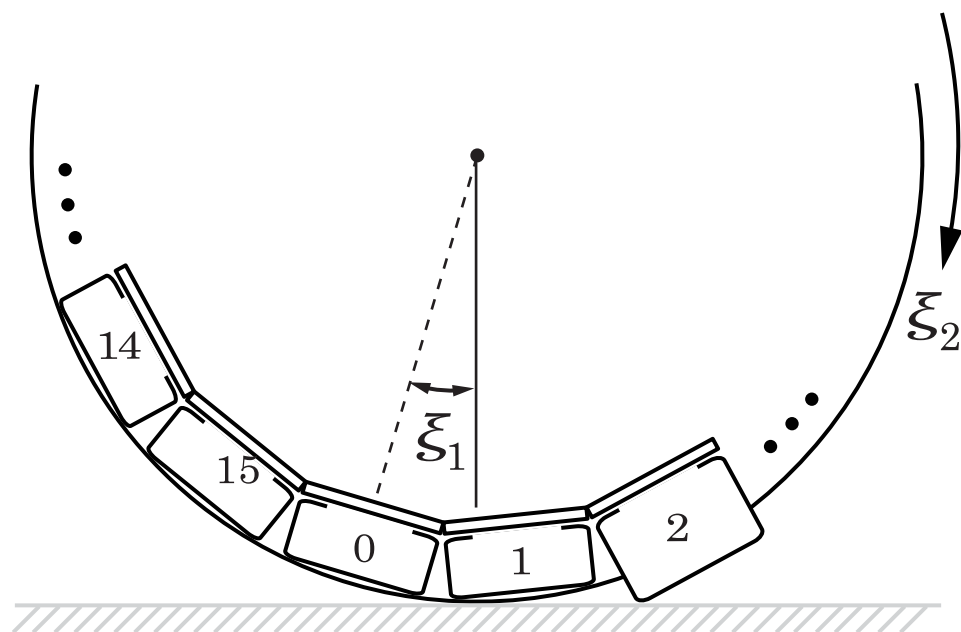


Step Tracking with Disturbance Estimator



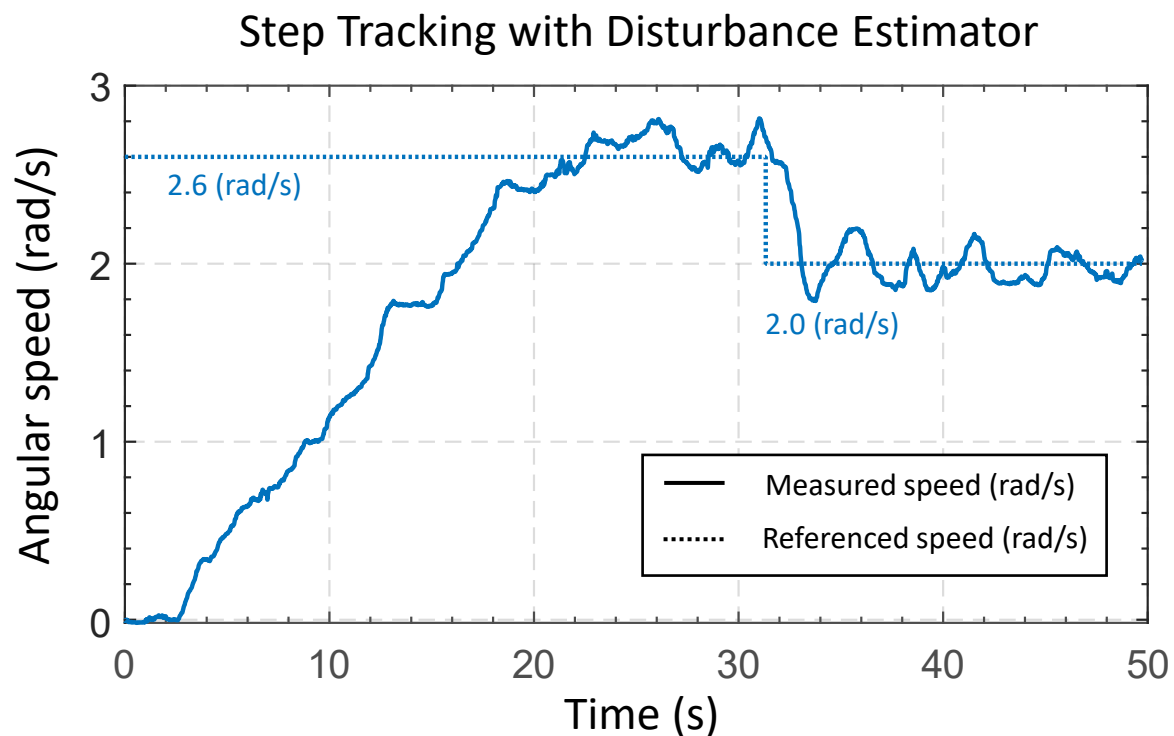
Ly, et. al. (In preparation)

### 3. Preliminary Results



Braking Input:

$$u = \begin{bmatrix} n_a = 16 \bmod (\eta + 2) \\ -22^\circ \\ -22^\circ < \varphi_d < 0 \end{bmatrix}$$



Ly, et. al. (In preparation)

## Summary of Contributions

**3 Firsts** of shell-bulging soft rolling robots:

- **The mobile embedded system** driven by electro-hydraulic actuators
- **The mathematical model**
- **The MPC-based controller** for speed regulation

## Future work

- Modeling and validating the actuation force functions for acceleration and braking
- Untethering the system with onboard power supply and controller.
- Redesigning into a spherical robot or adding an additional wheel-based robot with axle



Thank you

